The genetic Ca²⁺ sensor GCaMP3 reveals multiple Ca²⁺ stores differentially coupled to Ca²⁺ entry in the human malaria parasite *Plasmodium falciparum*

Lucas Borges-Pereira[1,2,‡], Samantha J. Thomas[2,‡], Amanda Laizy dos Anjos e Silva[3], Paula J. Bartlett[2], Andrew P. Thomas[2,*], and Célia R. S. Garcia[1,*]

From the ¹Departamento de Análises Clínicas e Toxicológicas, Faculdade de Ciências Farmacêuticas and the ³Departamento de Fisiologia, Instituto de Biociências, Universidade de São Paulo, São Paulo, Brasil, and the ²Department of Pharmacology, Physiology and Neuroscience, Rutgers University, New Jersey Medical School, Newark, New Jersey, USA

Edited by Roger J. Colbran

Cytosolic Ca²⁺ regulates multiple steps in the host-cell invasion, growth, proliferation, and egress of blood-stage *Plasmodium falciparum*, yet our understanding of Ca²⁺ signaling in this endemic malaria parasite is incomplete. By using a newly generated transgenic line of *P. falciparum* (PfGCaMP3) that expresses constitutively the genetically encoded Ca²⁺ indicator GCaMP3, we have investigated the dynamics of Ca²⁺ release and influx elicited by inhibitors of the sarcoplasmic/endoplasmic reticulum Ca²⁺-ATPase pumps, cyclopiazonic acid (CPA), and thapsigargin (Thg). Here we show that in isolated trophozoite phase parasites: (i) both CPA and Thg release Ca²⁺ from intracellular stores in *P. falciparum* parasites; (ii) Thg is able to induce Ca²⁺ release from an intracellular compartment insensitive to CPA; (iii) only Thg is able to activate Ca²⁺ influx from extracellular media, through a mechanism resembling store-operated Ca²⁺ entry, typical of mammalian cells; and (iv) the Thg-sensitive Ca²⁺ pool is unaffected by collapsing the mitochondria membrane potential with the uncoupler carbonyl cyanide *m*-chlorophenyl hydrazone or the release of acidic Ca²⁺ stores with nigericin. These data suggest the presence of two Ca²⁺ pools in *P. falciparum* with differential sensitivity to the sarcoplasmic/endoplasmic reticulum Ca²⁺-ATPase pump inhibitors, and only the release of the Thg-sensitive Ca²⁺ store induces Ca²⁺ influx. Activation of the store-operated Ca²⁺ entry–like Ca²⁺ influx may be relevant for controlling processes such as parasite invasion, egress, and development mediated by kinases, phosphatases, and proteases that rely on Ca²⁺ levels for their activation.

Malaria infection by *Plasmodium* parasites is responsible for a high rate of morbidity and mortality in humans, with over 200 million people infected and approximately half a million deaths annually. *Plasmodium falciparum* infection results in the most lethal form of malaria in humans and resistance to front line drugs is a growing issue (1). Fluctuations in the intracellular Ca²⁺ concentration plays a crucial role in controlling vital processes within mammalian cells such as fertilization, differ-

entiation, proliferation, and cell death (2). Similarly, key phases of the *Plasmodium* life cycle have been shown to depend on changes in Ca²⁺ concentration including intraerythrocytic parasite proliferation invasion and egress from the host cell, protein secretion, and cell-cycle regulation (3–12). Significantly, these Ca²⁺-signaling pathways can be coupled to extracellular ligands, including melatonin and ATP (4, 5, 10, 11). Advancing our understanding of the Ca²⁺ signaling pathways utilized in *P. falciparum* to trigger these essential processes has the potential to identify novel therapeutic targets.

Ca²⁺ ions inside the cell can bind to specific proteins or be sequestered within organelles. The endoplasmic/sarcoplasmic reticulum (ER/SR) is the major intracellular Ca²⁺ stores in mammalian cells and in most, although not all, eukaryotic cells (13). Ca²⁺ accumulation into the ER/SR depends on an ATP-driven Ca²⁺ pump named sarcoplasmic/endoplasmic reticulum Ca²⁺ ATPase (SERCA). In mammalian cells several isoforms of SERCA are expressed in different cells and ER/SR subcompartments, whereas Ca²⁺ accumulation in the Golgi and other post-Golgi, lumenally acidic organelles (secretory granules, lysosomes, post-Golgi vesicles), depends on the expression of different Ca²⁺ pumps, the so-called secretory pathway Ca²⁺ ATPases encoded by two genes, ATP2C1 and ATP2C2, and several spliced variants (14). Thg and CPA are known to be highly selective inhibitors of all mammalian SERCAs, whereas both drugs are totally ineffective on mammalian SPCAs (15). Only one poorly characterized inhibitor has been described for SPCA1, namely Bis(2-hydroxy-3-*tert*-butyl-5-methyl-phenyl)-methane (bis-phenol) (16, 17). Other mechanisms of Ca²⁺ accumulation in acidic compartments have been suggested to exist in mammalian cells, *e.g.* a H⁺/Ca²⁺ exchange mechanism, but based largely on indirect evidence (18, 19).

Evidence exists supporting the existence in most eukaryotes (and in some prokaryotes) of acidocalcisomes, intracellular compartments with an acidic lumen and containing large amounts of Ca²⁺ (and polyphosphates, in addition to Mg²⁺ and Zn²⁺). The histological nature of acidocalcisomes, however, is far from clear, and this term has been used to define different intracellular compartments, such as lysosomes, vacuoles, etc. (20). As to the mechanism of Ca²⁺ uptake, in unicellular organisms and particularly in trypanosomes, the most

convincing evidence is that acidocalcisomes are endowed with a plasma membrane type of Ca^{2+} ATPase (21).

The importance and relevant organelle(s) underlying Ca^{2+} stores in *P. falciparum* is still debated. Although most investigators agree on the importance of the ER as an inositol 1,4,5-trisphosphate (IP_3)–sensitive compartment, different results have been obtained concerning the acidic Ca^{2+} compartment (22). For example Biagini *et al.* (23) have suggested that in *P. falciparum* the digestive vacuole, in which hemoglobin is metabolized and degraded, represents the major dynamic acidic Ca^{2+} compartment of the cell. According to these authors, both Thg and CPA cause a drastic loss of Ca^{2+} from this organelle. On the contrary, an analysis with different fluorescent Ca^{2+} indicators by Rohrbach *et al.* (24) suggests that minor changes in the vacuole Ca^{2+} concentration occur upon addition of the two SERCA inhibitors. A major interpretation problem with all these studies is that the fluorescent Ca^{2+} indicators used are trapped not only in the cytosol or in specific organelles but also in cellular compartments, *i.e.* the cytosol, nucleus, ER, and digestive vacuole, which differ in terms of protein composition and luminal pH.

In mammalian cells a key tool to investigate the role of SERCA in Ca^{2+} signaling has been Thg, because of its high specificity in blocking selectively at low-nanomolar concentrations all SERCA isoforms. On the contrary, inhibition of *Plasmodium* SERCA (PfSERCA or PfATP6) by Thg is still debated. Data published by our group and others have shown that *Plasmodium* has a Thg-sensitive Ca^{2+} pump inhibited by the drug, albeit at higher concentrations than typically observed in mammalian cells (25–27). Other groups, on the contrary, have found no effect of Thg, including on saponin-isolated *Plasmodium* parasites (28). In a recent study published by Pandey *et al.* (29), the authors employed a transgenic line of *P. falciparum* expressing the Ca^{2+} sensor yellow cameleon–Nano, and in this work Thg and the antimalarial dihydroartemisinin also did not appear to affect cytosolic Ca^{2+}, whereas CPA was effective. Eckstein-Ludwig *et al.* (26) have employed heterologous expression of PfATP6 in *Xenopus* oocytes, and in their studies 0.8 μM Thg inhibited PfATP6 similarly to 1 μM CPA. However, employing the purified protein *in vitro*, Arnou *et al.* (30) showed that the IC_{50} of Thg for PfATP6 ATPase activity was $\sim$100 μM, much higher than for mammalian SERCA. By contrast, the IC_{50} for CPA acting on PfATP6 was actually $\sim$10-fold lower than for rabbit skeletal muscle SERCA1a.

Measurements of Ca^{2+} dynamics are usually performed by loading the cells with chemical fluorescent indicator dyes such as Fluo4 and Fura2. However, as shown by several groups (23, 24) (and mentioned above), these dyes are trapped not only in the cytosol but also in other cellular compartments, complicating the interpretation of the results and possibly explaining, at least in part, the discrepancy between the different published studies. To overcome this problem, we decided to utilize parasites expressing genetically encoded calcium indicators (GECIs) whose intracellular localization is highly selective in different cells, including protist parasites (29, 31, 32).

The GCaMP family, a group of GECIs derived from circularly permuted GFP with an engineered calmodulin inserted, was developed by Looger and co-workers (33). The GCaMP Ca^{2+} indicators offer improved photostability, increased brightness and dynamic range, and a range of affinities for Ca^{2+}, providing greatly enhanced signal to noise compared with FRET-based GECIs (33). The affinity of GCaMP3 for Ca^{2+} is 660 $\pm$ 19 nM, and it appears to be nontoxic even when constitutively expressed in living animals (34). We generated a *P. falciparum* (3D7) stably expressing GCaMP3 as a cytosol-located GECI, referred to as PfGCaMP3 (32). Using this approach, we have selectively monitored the changes of the cytosolic Ca^{2+} concentration ($[Ca^{2+}]_c$) in *P. falciparum* during different treatments to mobilize intracellular Ca^{2+} and activate Ca^{2+} influx. Given the exclusive localization in the cytoplasm of the Ca^{2+} probe used, the data presented are not contaminated by signals coming from other intracellular compartments that have plagued previous studies. Our studies show that both CPA and Thg increase the $[Ca^{2+}]_c$ in *P. falciparum* cells when added in the absence of extracellular Ca^{2+}, confirming that both drugs lead to Ca^{2+} discharge from intracellular Ca^{2+} pools. However, Thg appears to mobilize Ca^{2+} also from a pool not sensitive to CPA. Moreover, Thg but not CPA is able to activate Ca^{2+} influx in a process similar to store-operated Ca^{2+} entry (SOCE). The compartment sensitive only to Thg is unlikely to be the digestive vacuole, and it is clearly distinct from mitochondrion.

Results

PfGCaMP3 reveals that both CPA and Thg release Ca^{2+} from internal stores

In the past 20 years, a large body of work by us and others has employed chemical Ca^{2+} indicators trapped within the parasites using the intracellularly cleaved acetoxymethyl esters to characterize Ca^{2+}-signaling pathways in malaria parasites (5, 6, 35, 36). These dyes, however, are not exclusively located in the cytosol of *Plasmodium* spp. but are also trapped within organelles, with the relative distribution and localization depending on the experimental protocols and the strain utilized. More recently, we reported the generation of a new class of transgenic *P. falciparum* constitutively expressing the GECI GCaMP3 (PfGCaMP3) that could be employed to monitor selectively the dynamics of $[Ca^{2+}]$ only in the cytosol of the parasites (32). For all experiments described here, PfGCaMP3 cultures were synchronized by sorbitol treatment 12–16 h prior to the experiment, and then PfGCaMP3 parasites were isolated from the red blood cells with saponin. Fig. 1A shows the bright field, basal GCaMP3 fluorescence, and merged images of trophozoite parasites. The cultures were confirmed to be in the trophozoite phase using Giemsa smears (Fig. 1A) prior to isolation.

The ability of CPA and Thg to mobilize Ca^{2+} from intracellular stores has been studied *in vitro* by a number of groups, with varying results (26, 30): although the doses of CPA necessary for maximal Ca^{2+} release are similar to those used in mammalian cells, in *P. falciparum*, those of Thg are at least 1 order of magnitude higher than those employed in mammalian systems (25, 27–29). Kinetic measurements of CPA- and Thg-
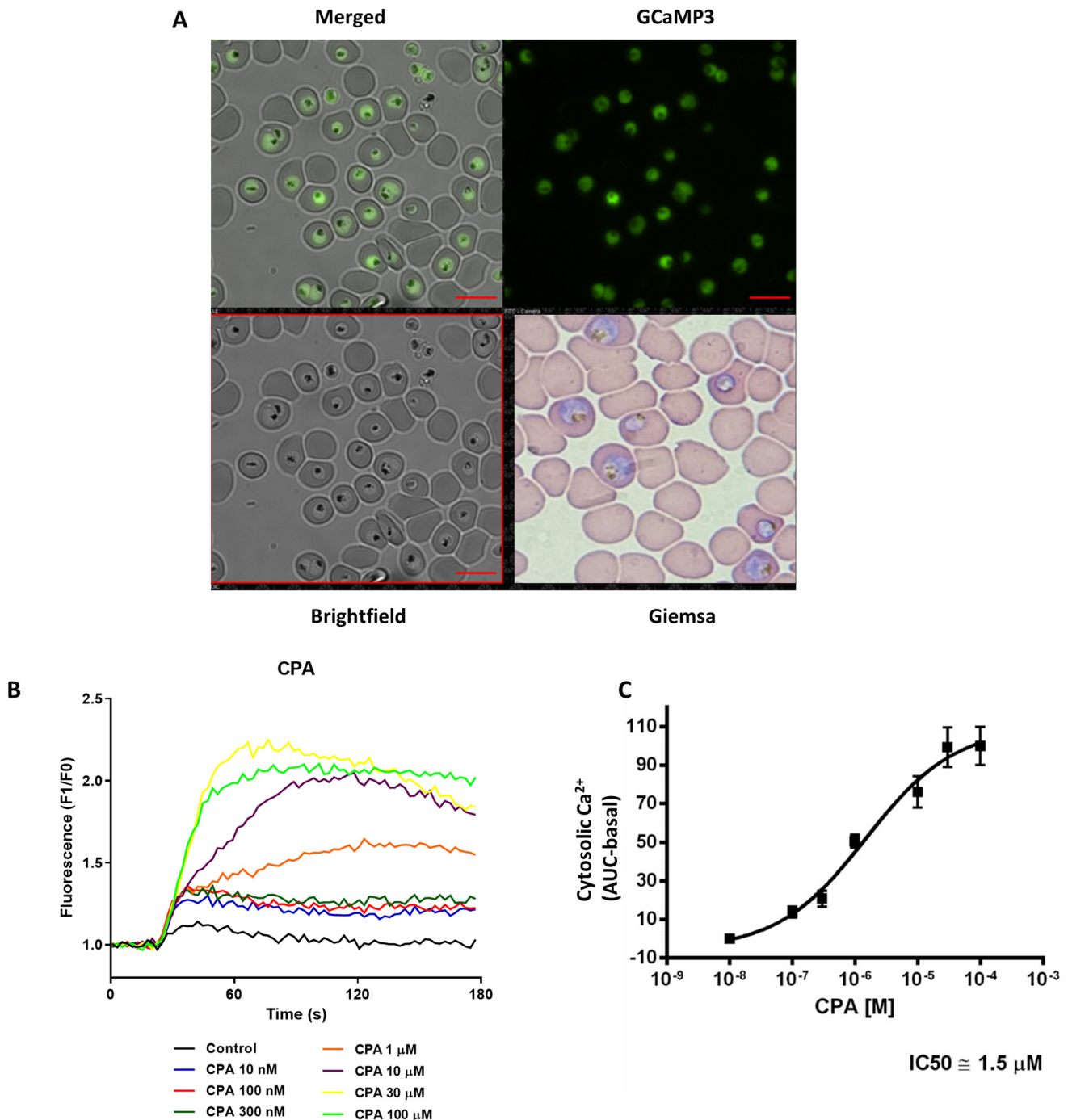
Figure 1. Measurement of [Ca^{2+}]$_c$ response of CPA with PfGCaMP3. A synchronized population of trophozoite-stage *P. falciparum* parasites expressing GCaMP3 (PfGCaMP3) were isolated, resuspended into MOPS buffer with 2 mM Ca^{2+}, and plated onto a 96-well black plate with a clear bottom (10^7 cells/well in 200 µl of total volume) pretreated with 50 µg/ml of poly-L-lysine. *A*, PfGCaMP3 parasites employed in the experiments. *B*, the Ca^{2+} dose response of isolated parasites to CPA was measured in a FlexStation 3 plate reader. *C*, the mean area under curve (*AUC*) of [Ca^{2+}]$_c$ in response to CPA was used to calculate the IC$_{50}$ value. *Scale bars*, 10 µM.

mediated Ca^{2+} rises in isolated PfGCaMP3 parasites immobilized on poly-L-lysine were carried out using a plate reader with microfluidic injection capabilities. This assay has advantages for throughput and small sample volume. Fig. 1*B* shows the dose-dependent effect of CPA to increase [Ca^{2+}]$_c$ (increased PfGCaMP3 fluorescence). The dose response to CPA revealed an IC$_{50}$ of 1.5 µM (Fig. 1*C*), consistent with previous studies. We have shown previously in isolated parasites that the maxi-

mal effect of Thg is obtained at ~25 µM (25). However, we were not able to accurately determine the IC$_{50}$ of Thg in the plate reader assay, because of the need to inject aqueous solutions at concentrations that exceed the solubility of Thg. However, at a final concentration of 1 µM, the rise in Ca^{2+} induced by Thg was equivalent to that caused by 10 nM CPA (data not shown), confirming that Thg is substantially less potent compared with mammalian cells, as discussed above (and see below).

CPA and Thg show differential effects on [Ca^{2+}]$_c$ in *P. falciparum*

To overcome the limitations of the plate reader assay, we utilized population measurements of isolated parasite suspensions in a fluorometer where Thg could be added directly from a concentrated DMSO stock solution (37). In this preparation the parasites are constantly stirred in the cuvette to prevent them from settling during the experiment, and this also allows rapid mixing of applied drugs, enabling us to test higher concentrations of Thg. In these experiments, in the presence of 2 mM CaCl$_2$ in the medium, CPA (30 μM) (Fig. 2A) and Thg (10 μM) (Fig. 2B) elicited a robust [Ca^{2+}]$_c$ increase in isolated PfGCaMP3 populations, with no change in [Ca^{2+}]$_c$ observed with vehicle control (Fig. 2C). However, the response to each drug was distinct; CPA caused a rapid [Ca^{2+}]$_c$ rise followed by a slowly declining phase, whereas Thg elicited an initial very rapid fluorescence increase, followed by a second slower rise and finally by a sustained, larger (compared with that caused by CPA) Ca^{2+} response that reached a plateau after ~200 s. Notably, the first rapid and small fluorescence rise caused by Thg is an artifact because it is also observed when Thg is added to a medium without cells (Fig. S1), so the quantitative data presented below were corrected for this artifact. Fig. 2D shows a summary of the peak Ca^{2+} data obtained in this series of experiments, all carried out in the presence of extracellular Ca^{2+}.

To determine whether Ca^{2+} influx across the plasma membrane contributes to the Thg response, we repeated the experiments in the absence of extracellular Ca^{2+} (Fig. 2, E–G). Under these conditions the transient CPA response was similar to that in the presence of extracellular Ca^{2+}, whereas the sustained phase of the Thg response was abolished. Thus, it appears that there is a significantly larger Thg-induced [Ca^{2+}]$_c$ rise only in the presence of Ca^{2+} in the medium (Fig. 2H).

In mammalian cells, Ca^{2+} release from the ER is often followed by Ca^{2+} entry across the plasma membrane into the cytosol, by a process described as SOCE. The usual protocol to reveal SOCE in mammalian cells is to treat the cells with Thg or CPA in Ca^{2+}-free medium to empty the intracellular Ca^{2+} stores, followed by the readdition of Ca^{2+} to the medium. When SOCE is activated, Ca^{2+} readdition results in a large and sustained increase in [Ca^{2+}]$_c$. Ca^{2+} add-back in the experiments of Fig. 2 (E–G) resulted in an increase in [Ca^{2+}]$_c$ that was much larger after Thg treatment than with CPA or the DMSO control. These data are summarized in Fig. 2I and suggest that in *P. falciparum* some form of SOCE appears to be selectively activated by Thg but not by CPA.

Thg but not CPA targets an intracellular Ca^{2+} pool that is linked to SOCE

Based on *in vitro* evidence (30), the pharmacological target of both CPA and Thg is assumed to be PfATPase6. However, because these two drugs appear to have differential effects on SOCE in *P. falciparum*, we decided to investigate whether other *Plasmodium* Ca^{2+} pumps, in common or distinct intracellular Ca^{2+} pools, could be targeted by the drugs. To determine whether CPA and Thg release Ca^{2+} from the same pool, we

investigated whether Thg and CPA interfere with the Ca^{2+} response of each other by adding the two SERCA inhibitors in sequence (Fig. 3). The addition of Thg abolished the Ca^{2+} rise elicited by subsequent CPA addition, in both the presence and the absence of extracellular Ca^{2+} (Fig. 3, A and B). By contrast, pretreatment with CPA only partially reduced the Ca^{2+} response to subsequent Thg addition (Fig. 3, C and D). As expected, no [Ca^{2+}]$_c$ rise was observed after addition of the DMSO solvent control (Fig. 3, E and F). These data are summarized in Fig. 3 (G and H). Significantly, when Ca^{2+} was added back to cells incubated in the absence of extracellular Ca^{2+} (Fig. 3, B, D, and F), Ca^{2+} influx was activated whether Thg was added before or after CPA, and these data are also summarized in Fig. 3H. One interpretation of these findings is that there are two Ca^{2+} pools: one sensitive to both CPA and Thg and the other sensitive to only Thg. However, as noted under "Discussion," it is also possible that CPA and Thg differentially target distinct Ca^{2+} pumps in a single organelle.

Single-cell measurements suggest that Thg targets an additional Ca^{2+} pool

Population measurements of CPA- and Thg-induced GCaMP3 signal changes in a large number of cells provide robust and reproducible data; however, we wanted to confirm that the effects we report above are occurring in the same cell and not in two distinct cell populations. To this aim, trophozoite stage PfGCaMP3 parasites were saponin-isolated as above and then immobilized onto borosilicate glass coverslips with Cell-Tak. GCaMP3 images (excitation, 488 nm; emission, 510 nm) were collected at 1 Hz on a wide-field epifluorescent microscope at 37 °C. Because individual PfGCaMP3 cells differ in expression levels and basal signals are low, the single-cell imaging traces were normalized to the peak signal obtained with 10 μM ionomycin in the presence of 2 mM extracellular Ca^{2+} (Fig. 4).

Consistent with the population data collected in the fluorometer shown in Fig. 2, CPA elicits a robust, transient [Ca^{2+}]$_c$ response (Fig. 4B), whereas no [Ca^{2+}]$_c$ rise was observed in the solvent control (Fig. 4A). However, in this type of single-cell imaging experiments, we observed that Thg elicits a markedly different [Ca^{2+}]$_c$ response pattern characterized by a delay of several minutes followed by fast, oscillatory behavior of variable frequency (Fig. 4C). By contrast, Ca^{2+} oscillations were never observed with CPA. As to the time-to-response discrepancy between CPA and Thg effects in single-cell imaging and population measurements, we believe that this again reflects the lower solubility of Thg, and the time taken for Thg diffusion into the cells. In this setup Thg could not be added through a perfusion system because the drug binds strongly to the plastic tubes and never reaches an effective concentration in the cells. These problems do not occur in the cuvette of the fluorometer thanks to the constant rapid mixing in these experiments. Individual Ca^{2+} oscillations are not observed in the population experiments with the fluorimeter because they are not synchronous; thus, as expected, the mean trace data of all cells in the imaging field yield a similar monophasic sustained Ca^{2+} increase, albeit much slower than in the stirred cuvette system
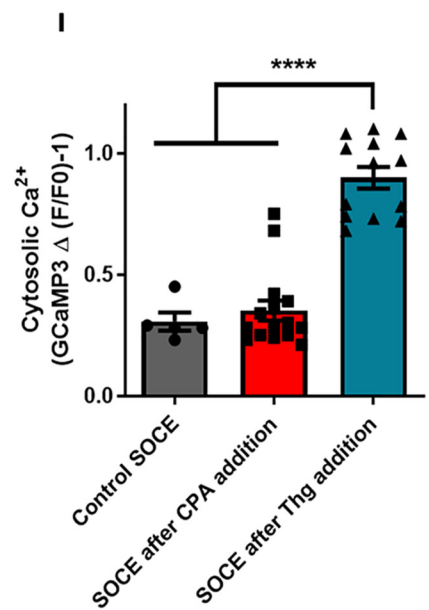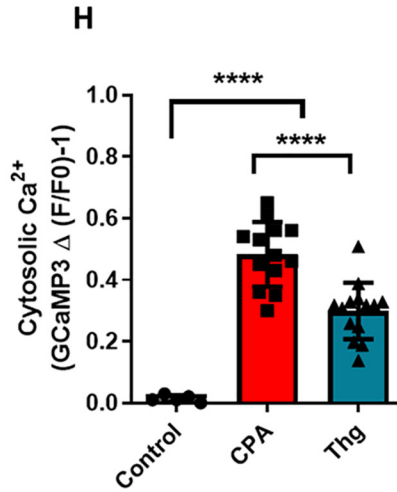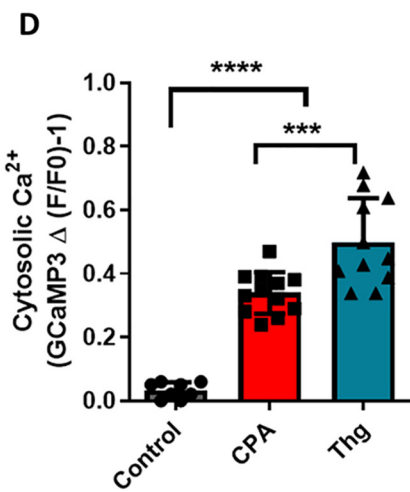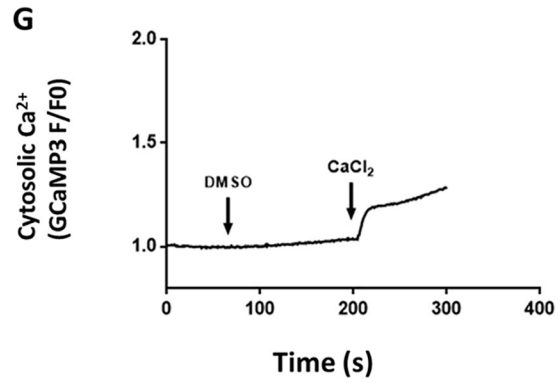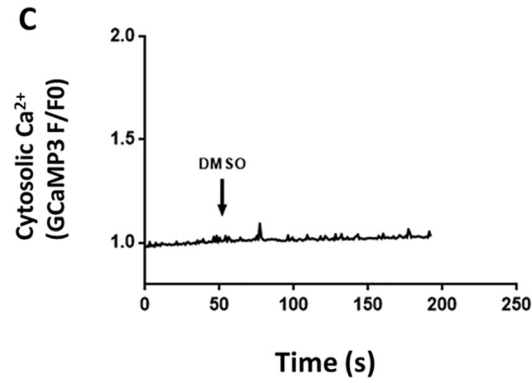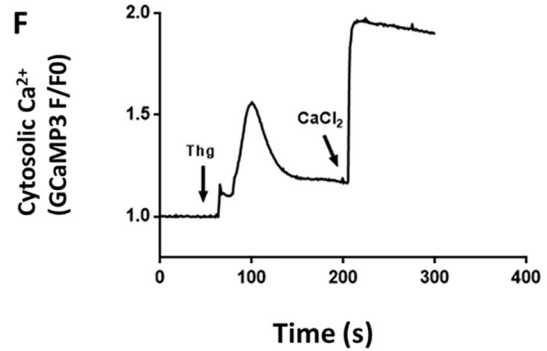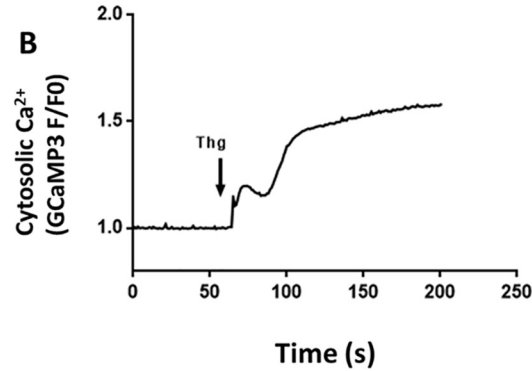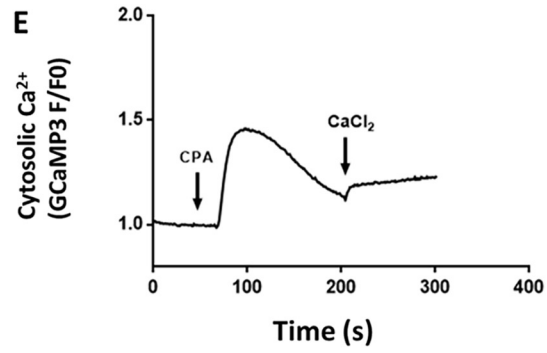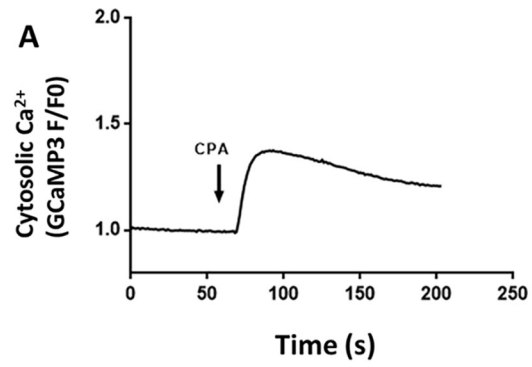
(Fig. S2). The time lag between Thg addition and onset of response may account for some discrepancies in the literature in which Thg is reported not to act in *P. falciparum* (29).

We also performed single-cell imaging experiments in Ca^{2+}-free buffer supplemented with 100 μM EGTA that confirmed the population data showing that only Thg, but not CPA, induces SOCE in *P. falciparum*. CPA and Thg gave similar response patterns under Ca^{2+}-free conditions (Fig. 4, *D–F*); however, only Thg was able to trigger Ca^{2+} entry into the cell following the addition of 2 mM CaCl$_2$ into the buffer. Both the amplitude (Fig. 4*G*) and rate of [Ca^{2+}]$_c$ increase (Fig. 4*H*) on Ca^{2+} addition following Thg treatment were significantly greater than with CPA or vehicle control. The amplitude was 2-fold larger following Thg compared with CPA, and the rate of rise of [Ca^{2+}]$_c$ was 6-fold faster. The response to Ca^{2+} add-back following CPA was not significantly different from that observed in the vehicle control, but both rates were relatively rapid. This reflects a constitutive Ca^{2+} entry component in these cells, which is demonstrated by the similar amplitude decrease of [Ca^{2+}]$_c$ when extracellular Ca^{2+} is removed (Fig. S3).

The interactions between CPA and Thg were further investigated at the single-cell level. For these experiments, sequential additions of both drugs were performed in the presence of 2 mM extracellular Ca^{2+}. When CPA was added first, Thg was still able to elicit a [Ca^{2+}]$_c$ response, which was typically oscillatory in nature (Fig. 5*A*). However, when Thg was added first, the addition of CPA failed to further increase [Ca^{2+}]$_c$ (Fig. 5*B*). We found that on average 80% of cells responded to both drugs when CPA was added first, whereas only 20% of cells responded to both drugs when Thg was added first (Fig. 4*C*). In the latter experiments the residual response to CPA could be because the slow onset Thg response had yet to fully release the Ca^{2+} store.

Other Ca^{2+} stores

A variety of evidence suggests that in *P. falciparum* the ER represents a major Ca^{2+} storage compartment endowed with a unique IP$_3$-sensitive Ca^{2+} release channel (5, 11, 36, 38). Additional Ca^{2+} stores have been identified in *P. falciparum* that may contribute to cytosolic Ca^{2+} dynamics, including an acidic Ca^{2+} pool and the mitochondrion (22). The most abundant acidic compartment in *Plasmodium* is the digestive vacuole in which hemoglobin is metabolized (39). It has been proposed that the digestive vacuole can act as a dynamic Ca^{2+} storage organelle, playing a major role in maintaining *P. falciparum* Ca^{2+} homeostasis and redistributing Ca^{2+} during parasite growth and development (23). However, other groups have argued that the free Ca^{2+} in the vacuole is too low to significantly contribute to Ca^{2+} release in response to stimulation (24). A classical approach to investigate the presence and role of acidic compartments is that of collapsing their luminal pH.

To investigate whether an acidic compartment is the additional Thg-sensitive Ca^{2+} pool, we used the K$^+$/H$^+$ ionophore nigericin (Nig), which results in the release of Ca^{2+} from acidic compartments, including the digestive vacuole, by abolishing the pH gradient. Single-cell imaging experiments with isolated PfGCaMP3 parasites were performed in Ca^{2+}-free medium to ensure that [Ca^{2+}]$_c$ responses were due to intracellular stores and not Ca^{2+} influx across the plasma membrane. Addition of 250 nM Nig resulted in a large and rapid [Ca^{2+}]$_c$ increase detected by GCaMP3 (Fig. 6*A*, *green trace*). The [Ca^{2+}]$_c$ increase was preceded by a transient decrease in GCaMP3 fluorescence, which likely reflects acidification of the cytosol. This acidification would tend to decrease the Ca^{2+} sensitivity of GCaMP3, so the relatively large [Ca^{2+}]$_c$ increase with Nig indicates that there is a large acidic pool, most likely the digestive vacuole. As noted above, the isolated parasites have a constitutive Ca^{2+} influx pathway, which may preload the intracellular Ca^{2+} stores because they are prepared in 2 mM extracellular Ca^{2+}. Therefore, to be sure the GCaMP3 signal was not too close to saturation to observe differences in Ca^{2+} release to CPA or Thg, the PfGCaMP3 parasites were co-loaded with the lower-affinity ratiometric Ca^{2+} indicator Fura-FF (5 μM Fura-FF/AM for 1 h) prior to imaging both Ca^{2+} indicators simultaneously, as described under "Experimental procedures."

The *blue traces* of Fig. 6 (*A–C*) show the Fura-FF fluorescence ratio measured with 340- and 380-nm excitation recorded at the same time as the *green traces* of GCaMP3 fluorescence excited at 488 nm; all were detected with 510-nm emission. The lower-affinity Fura-FF signals show slower kinetics and lower amplitude relative to the maximum [Ca^{2+}]$_c$ after ionomycin. Nevertheless, both indicators reported the [Ca^{2+}]$_c$ transient elicited by CPA (Fig. 6*B*) and the delayed [Ca^{2+}]$_c$ oscillations following Thg addition (Fig. 6*C*), as well as the large amplitude Nig-induced [Ca^{2+}]$_c$ elevations. Because the Fura-FF signals were clearly not saturated, they were used to quantitate the effect of CPA and Thg on the Ca^{2+} response to Nig. Neither agent reduced the amplitude of the Nig-induced [Ca^{2+}]$_c$ increase as compared with the vehicle control (Fig. 6*D*), suggesting that they do not act on the main acidic pool in *P. falciparum*. It was more difficult to quantitate the relatively small responses to CPA and Thg added after Nig, but both agents elicited [Ca^{2+}]$_c$ increases in the presence of Nig (Fig. 6*E*). It has been shown that the *P. falciparum* mitochondrion can also act as a dynamic intracellular Ca^{2+} store and participates in Ca^{2+} homeostasis (40). To investigate whether the mitochondrion is involved in Thg-mediated Ca^{2+} release, we utilized the mitochondrial uncoupler carbonyl cyanide *m*-chlorophenyl hydrazine (CCCP). We first confirmed the required dose needed to collapse the mitochondrial membrane potential by adding CCCP to isolated parasites loaded with the membrane potential

Figure 2. SOCE is activated by Thg but not by CPA in *P. falciparum* parasites. Isolated PfGCaMP3 parasites at the trophozoite stage were placed in a 1-ml stirred cuvette at a density of 10^7 cells ml^{-1} and maintained at 37 °C. Changes in [Ca^{2+}]$_c$ were detected using a Shimadzu spectrofluorometer (RF5301PC, Japan), with excitation of 488 nm and emission of 530 nm. Representative traces of cytosolic Ca^{2+} dynamics after addition of the compounds, 30 μM CPA, 10 μM Thg, or DMSO as control are shown in the presence (*A–C*) and absence (*E–G*) of extracellular Ca^{2+} (no CaCl$_2$ added plus addition of 100 μM EGTA). In the presence of 2 mM Ca^{2+}, Thg elicits a prolonged [Ca^{2+}]$_c$ response with larger maxima than CPA (*D*). Removal of extracellular Ca^{2+} did not reduce the response to CPA, whereas the Thg response was smaller in the absence of extracellular Ca^{2+} (*H*). Peak [Ca^{2+}]$_c$ after add-back of extracellular Ca^{2+} (*E–G*) was elevated above the control with Thg but not with CPA (*I*). The data in *D*, *H*, and *I* are the means ± S.D. from three or more independent experiments, with individual data points shown. Statistical significance was calculated by one-way ANOVA with Bonferroni's multiple comparison test. ***, *p* = 0.009; ****, *p* < 0.001.
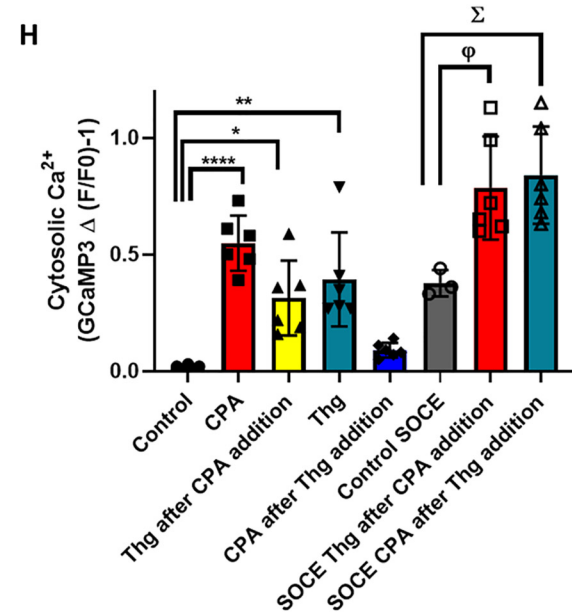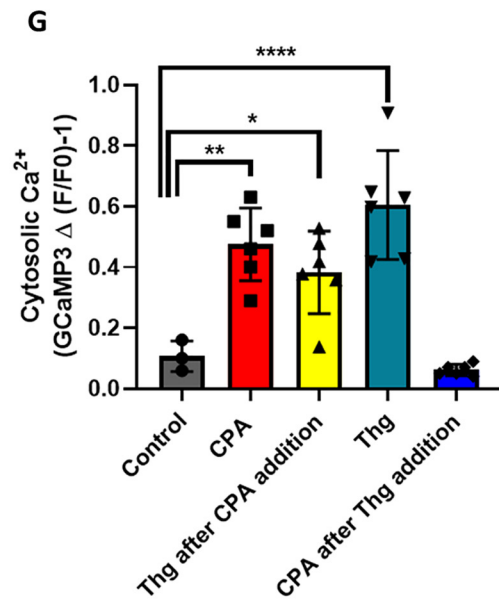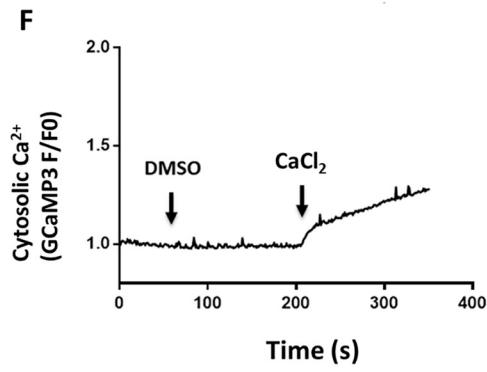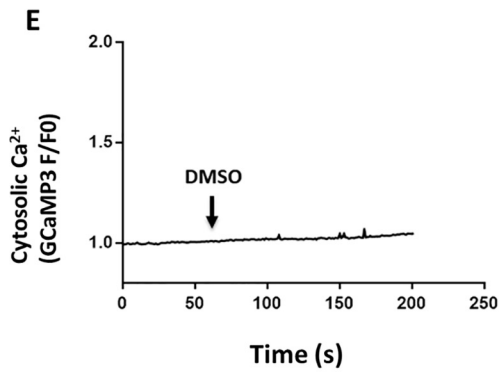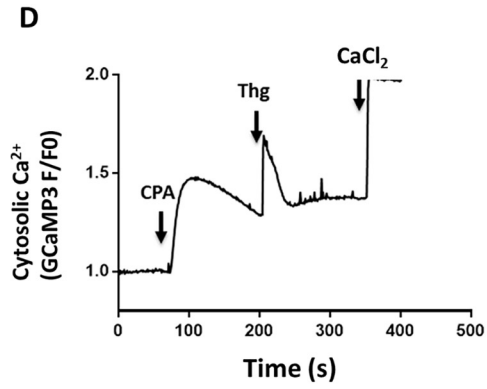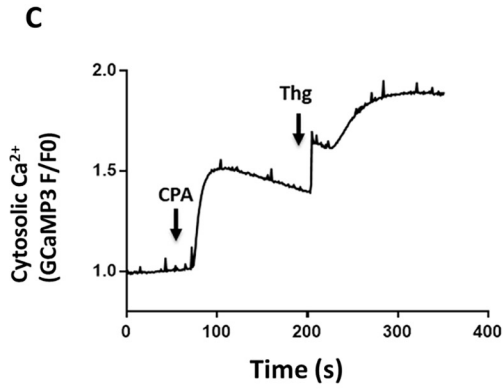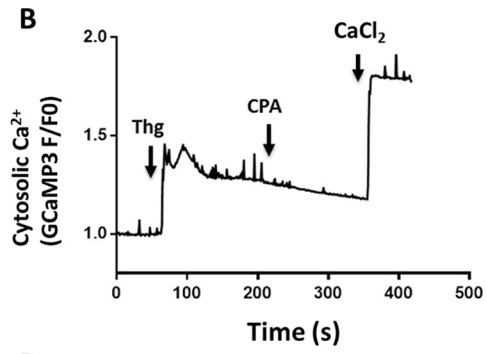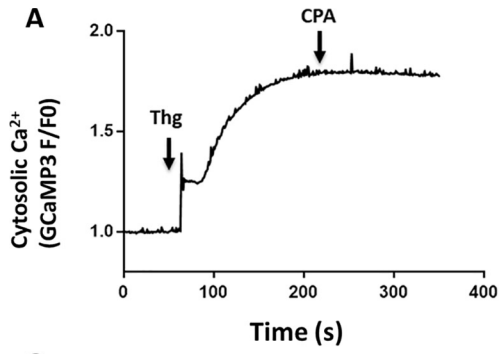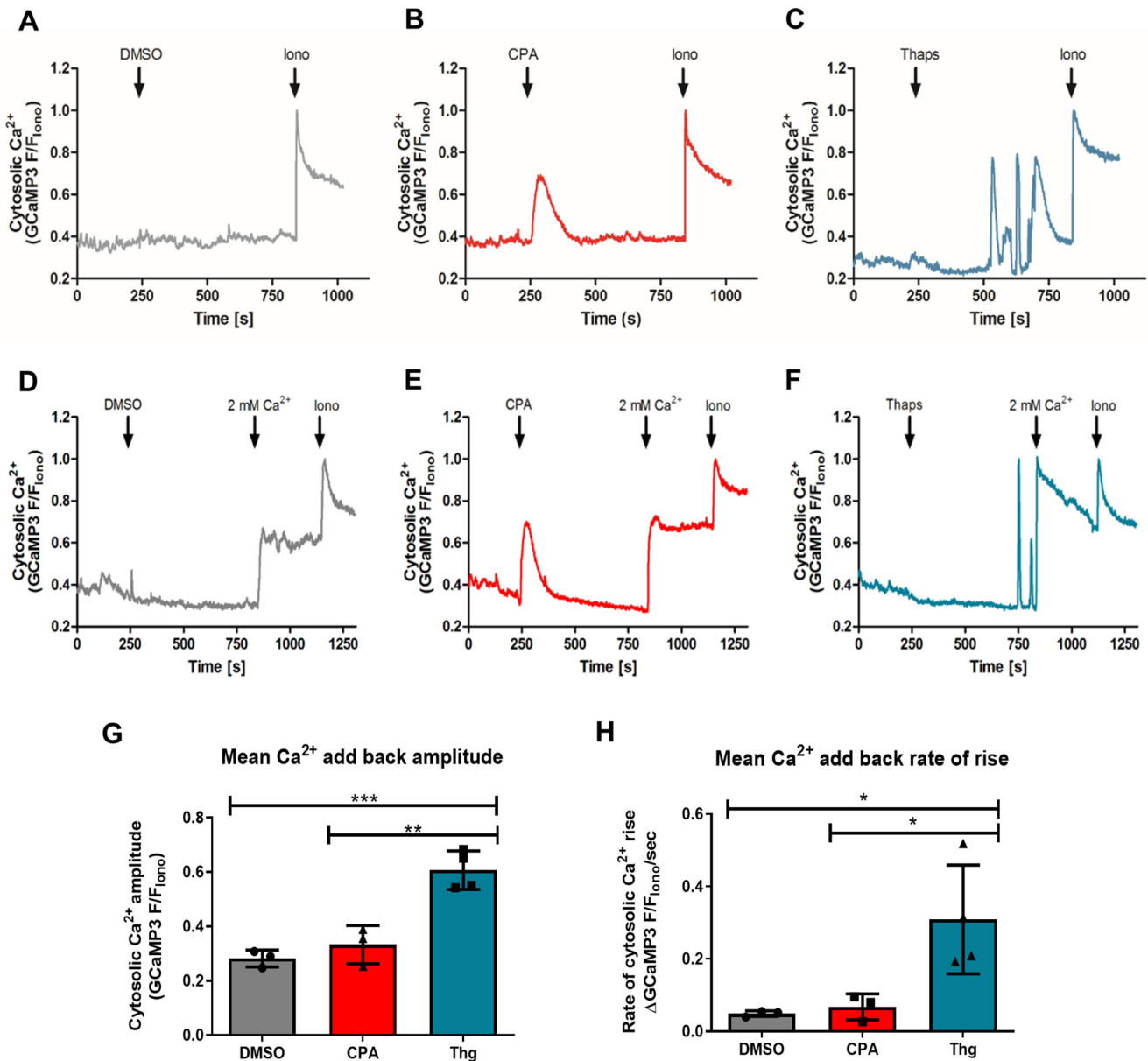
Figure 4. The ability of Thg but not CPA to induce SOCE is confirmed at the single-cell level. Synchronized trophozoite-stage PfGCaMP3 parasites were isolated, resuspended into MOPS buffer with 2 mM CaCl₂, and plated onto glass coverslips. The cell chamber was mounted on an epifluorescence microscope, and GCaMP3 images (excitation, 488 nm; emission, 510 nm; long band pass filter) were acquired at 1 Hz. Shown are representative traces of changes in $[Ca^{2+}]_c$ in the presence of extracellular Ca^{2+} in response to DMSO control (*A*), 10 μM CPA (*B*), and 5 μM Thg (*C*). The Ca^{2+} ionophore ionomycin (10 μM, *Iono*) was added at the end of each experiment. To assess SOCE after CPA and Thg addition, the buffer was switched to Ca^{2+}-free MOPS buffer with 100 μM EGTA immediately prior to recording. The cells were then treated with DMSO (*D*), 10 μM CPA (*E*), or 5 μM Thg (*F*) for 10 min prior to CaCl₂ addition (2 mM). All responses were normalized to the peak signal with 10 μM ionomycin (F/F_{Iono}). The amplitude (*G*) and rate of $[Ca^{2+}]_c$ rise (*H*) in response to CaCl₂ addition was significantly greater than the vehicle control following treatment with Thg, but not CPA. The data in *G* and *H* were averaged from at least 15 cells in each experiment and are the means ± S.D. from three or more independent experiments. In *G*, **, $p = 0.0053$; ##, $p = 0.0082$. In *H*, *, $p = 0.0345$; #, $p = 0.0483$ one-way ANOVA with Bonferroni's multiple comparison test.

dye tetramethylrhodamine ethyl ester (TMRE). We found that 2.5 μM CCCP (added with 2.5 μgml⁻¹ oligomycin to prevent reversal of the mitochondrial ATP synthase) uncoupled the mitochond-rion and caused the maximum decrease in the TMRE signal within the parasite (Fig. 7*A*). We then treated isolated PfGCaMP3 parasites with the same dose of CCCP/oligomycin to uncouple

Figure 3. Thg releases Ca²⁺ from more than one compartment in *P. falciparum* parasites. $[Ca^{2+}]_c$ was monitored in isolated PfGCaMP3 parasites at the trophozoite stage suspended in the cuvette of a spectrofluorometer, as described in the legend of Fig. 2. The PfGCaMP3 parasites were sequentially exposed to 10 μM Thg then 30 μM CPA (*A* and *B*), CPA then Thg (*C* and *D*), or DMSO control (*E* and *F*) in the presence (*A*, *C*, and *E*) or absence (*B*, *D*, and *F*) of extracellular Ca^{2+} (no CaCl₂ added plus addition of 100 μM EGTA). The CPA Ca^{2+} response was blocked after Thg addition (*A* and *B*); however, the Thg Ca^{2+} response was not abolished by CPA (*C* and *D*). *A–F* are representative traces. The mean peak Ca^{2+} response to each drug addition is plotted in the presence (*G*) or absence (*H*) of extracellular Ca^{2+}. The data are the means ± S.D. from three or more independent experiments with individual data points shown. Statistical significance was calculated by one-way ANOVA with Bonferroni's multiple comparison test. In *G*, *, $p = 0.017$; **, $p = 0.0013$; ****, $p < 0.0001$. In *H*, *, $p = 0.0256$; **, $p = 0.0035$; ****, $p < 0.0001$; φ, $p = 0.0257$; Σ, $p = 0.0124$.
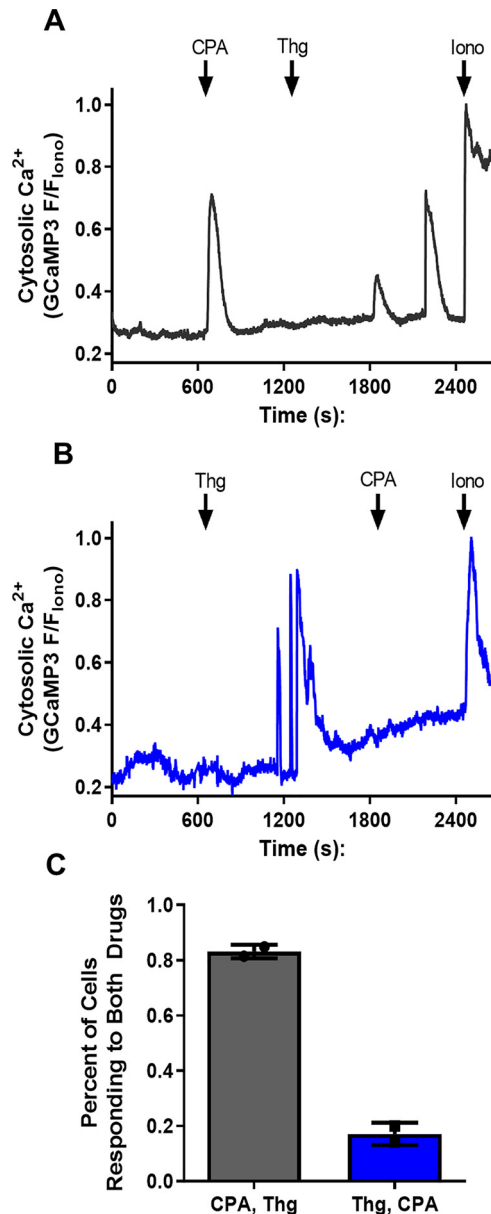
Figure 5. Thg blocks the CPA [Ca^{2+}]$_c$ response, but CPA does not block the Thg [Ca^{2+}]$_c$ response in single *P. falciparum* trophozoites. Synchronized PfGCaMP3 parasites were isolated, resuspended into HEPES buffer with 2 mM CaCl$_2$, and plated on glass coverslips before loading into the incubation chamber of an epifluorescence microscope to image GCaMP3. The cells were treated with sequential additions of 10 μM CPA and 5 μM Thg as indicated (*A* and *B*) to determine whether the addition of either drug interfered with the ability of the other to mobilize Ca^{2+}. Responses were normalized to the peak ionomycin (10 μM, *Iono*) response (*F/F*$_{Iono}$), and the percentage of cells responding to both drugs was measured (*C*). The data are the means from ≥127 cells ± S.D. from two independent experiments.

the mitochondrion before adding CPA followed by Thg (Fig. 7*B*). Mitochondrial uncoupling did not cause any Ca^{2+} release on its own and did not affect the ability of either CPA or Thg to elicit a [Ca^{2+}]$_c$ response. After treatment with CCCP/oligomycin, 76.5 ± 1.6% of cells responded to Thg, similar to the 85.0 ± 9.6% of cells responding to Thg in controls (means ± S.E., *n* = 3). These data indicate that the parasite mitochondrion does not contribute to the additional source of Thg-induced Ca^{2+} release.

Discussion

We and other groups have demonstrated that *Plasmodium* parasites have ER-like internal Ca^{2+} pools sensitive to Thg and CPA, as well as an acidic Ca^{2+} pool that can be released with nigericin or chloroquine (5, 6, 25, 26, 30, 41). In higher eukaryotes, Ca^{2+} efflux from the ER is mediated by IP$_3$ or ryanodine receptors. We have described IP$_3$-dependent Ca^{2+} release in asexual stages of *P. falciparum* and *Plasmodium chabaudi* parasites (38, 41), including in the intraerythrocytic parasite using caged IP$_3$ (5). The production of IP$_3$ and diacylglycerol has also been reported during *Plasmodium* gametogenesis, a fundamental step in parasite transmission to the mosquito vector (42). These findings support the conclusion that *Plasmodium* relies on Ca^{2+} signaling for its survival in the vertebrate and invertebrate hosts.

Experiments with intracellularly trappable chemical Ca^{2+} indicators are plagued by the partial localization of the dyes in different compartments caused by compartmentalization into organelles. This problem appears to be particularly relevant in *Plasmodium* spp., where there is a prominent accumulation into the digestive vacuole in the absence of anion transport inhibitors (23). Thus, there is always the possibility that changes in Ca^{2+} concentration measured with chemical Ca^{2+} indicators loaded into cells as the acetoxymethyl ester could reflect, at least in part, events not occurring in the cytoplasm. On the contrary, with GECIs, the localization of the expressed Ca^{2+} indicator protein is highly specific and, in the case of our GCaMP3-expressing *P. falciparum* (PfGCaMP3), exclusively in the cytoplasm. Not only is the GCaMP3 specifically targeted to the cytoplasm, but because of its relatively low affinity for Ca^{2+} compared with chemical indicators such as Fura2, and its lower diffusion rate, it has a reduced Ca^{2+} buffering capacity and less effect on the spatial dynamics of Ca^{2+} within the cell.

Here we show unambiguously, by using the PfGCaMP3 parasites, that in *P. falciparum* both SERCA inhibitors, Thg and CPA, are capable of releasing Ca^{2+} from intracellular stores into the cytoplasm of the parasites. The IC$_{50}$ of CPA was determined to be 1.5 μM, a concentration that was in a similar range to that usually found in mammalian cells. However, in contrast to mammalian cells where Thg is typically observed to be more potent than CPA, our studies with PfGCaMP3 show that higher concentrations of Thg are required, consistent with other studies of the effects of Thg in *Plasmodium* spp. (25–27, 30). The low solubility of Thg makes it difficult to perform dose-response studies in the high concentration range required for maximal effect, but in previous studies with isolated *P. falciparum* parasites (loaded with Fluo-3 and analyzed by confocal microscopy), we observed a maximum Ca^{2+} release response at 25 μM Thg (25). This falls within the broad concentration range reported for inhibition of the Ca^{2+}-ATPase activity of purified or heterologously expressed PfATP6 (26, 30). Using the GECI yellow cameleon–Nano in *P. falciparum* parasites, Pandey *et al.* (29) reported that there was no response to Thg (7.6 μM) in imaging experiments under conditions where they could observe a CPA-induced [Ca^{2+}]$_c$ increase. However, the low signal-to-noise obtained using this FRET-based Ca^{2+} indicator required averaging of data across many cells from multiple
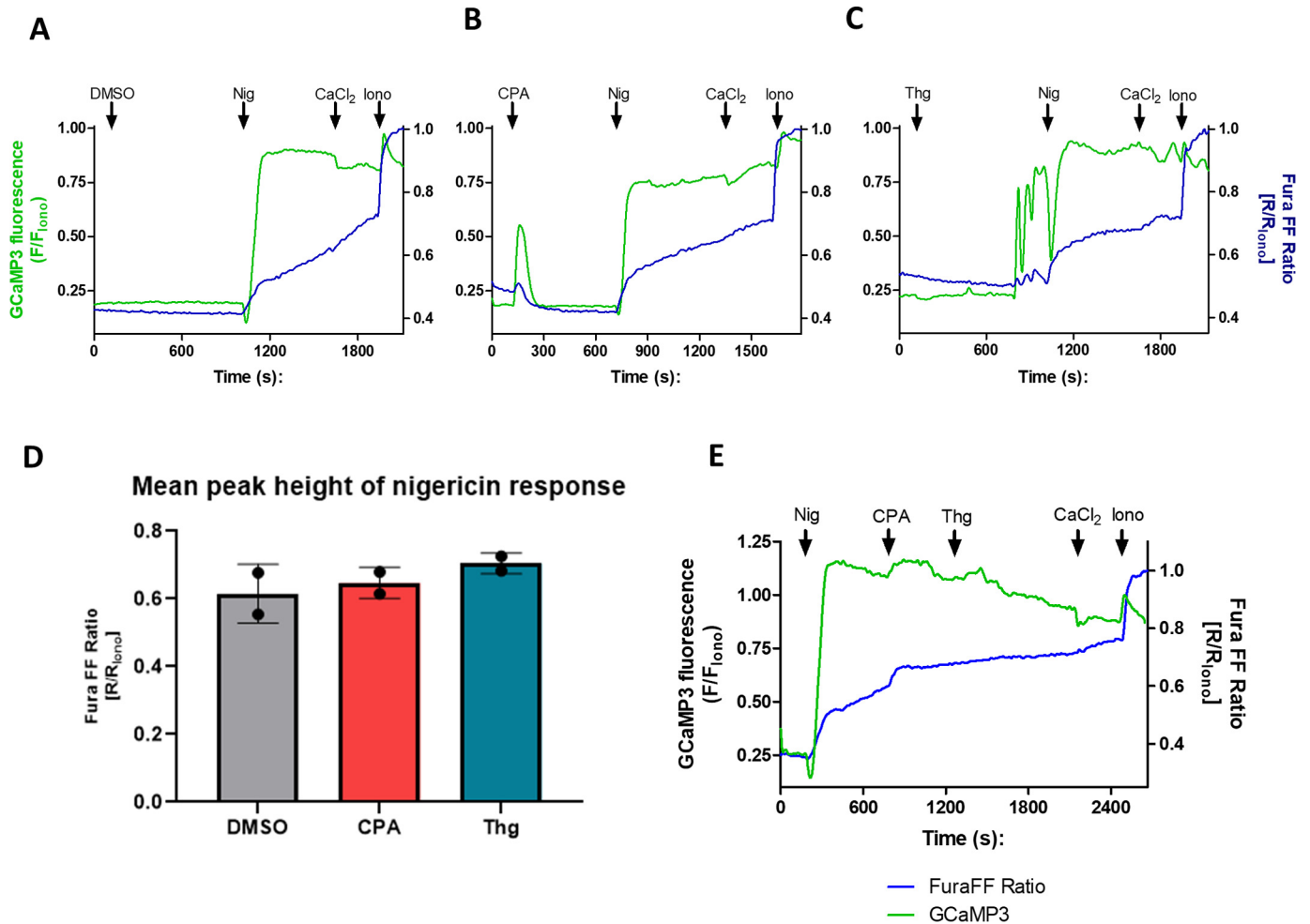
Figure 6. The major acidic compartment is not affected by Thg or CPA. Isolated PfGCaMP3 parasites synchronized at the trophozoite stage were loaded with 5 μM Fura-FF/AM for 1 h while plating onto glass coverslips. The dual-loaded cells were transferred to the microscope imaging chamber, and immediately prior to recording, the buffer was switched to Ca^{2+}-free MOPS buffer with 100 μM EGTA. The images were acquired at 1 Hz for both GCaMP3 (excitation, 488 nm; emission, 510 nm) and Fura-FF (excitation, 340 and 380 nm; emission, 510 nm). The cells were treated with either the DMSO vehicle control (*A*), 10 μM CPA (*B*), or 5 μM Thg (*C*) for 10–15 min, and then Nig (250 nM) was added for another 10 min prior to adding back 2 mM $CaCl_2$ followed by 10 μM ionomycin (*Iono*). GCaMP3 fluorescence and the Fura-FF 340 nm/380 nm fluorescence ratio were normalized to the peak ionomycin (10 μM) response. The mean peak height of the Nig Ca^{2+} response was unaffected by CPA or Thg (*D*). Nigericin does not prevent a subsequent response to CPA and Thg (*E*). The data are the means ± S. D. of ≥60 cells from two independent experiments.
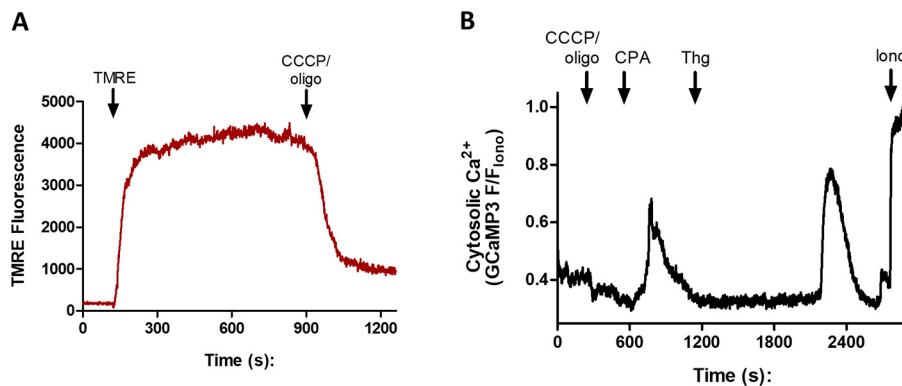

Figure 7. Mitochondria uncoupling does not affect [Ca²⁺]$_c$ responses to CPA or Thg. Synchronized PfGCaMP3 parasites were isolated, resuspended into MOPS buffer with 2 mM $CaCl_2$, plated onto glass coverslips, and loaded into the incubation chamber of an epifluorescence microscope. The cells were loaded with 5 nM TMRE and then treated with 2.5 μM CCCP plus 2.5 μg/ml oligomycin (*oligo*), which uncouples the mitochondria (*A*). TMRE fluorescence was monitored with 543-nm excitation and 580-nm emission. In *B*, GCaMP3 images were acquired at 1 Hz (excitation, 488 nm; emission, 510 nm), and the cells were treated sequentially with CCCP plus oligomycin, 10 μM CPA, and 5 μM Thg. GCaMP3 signals were normalized to the peak ionomycin (10 μM, *Iono*) response (*F/F_{Iono}*).
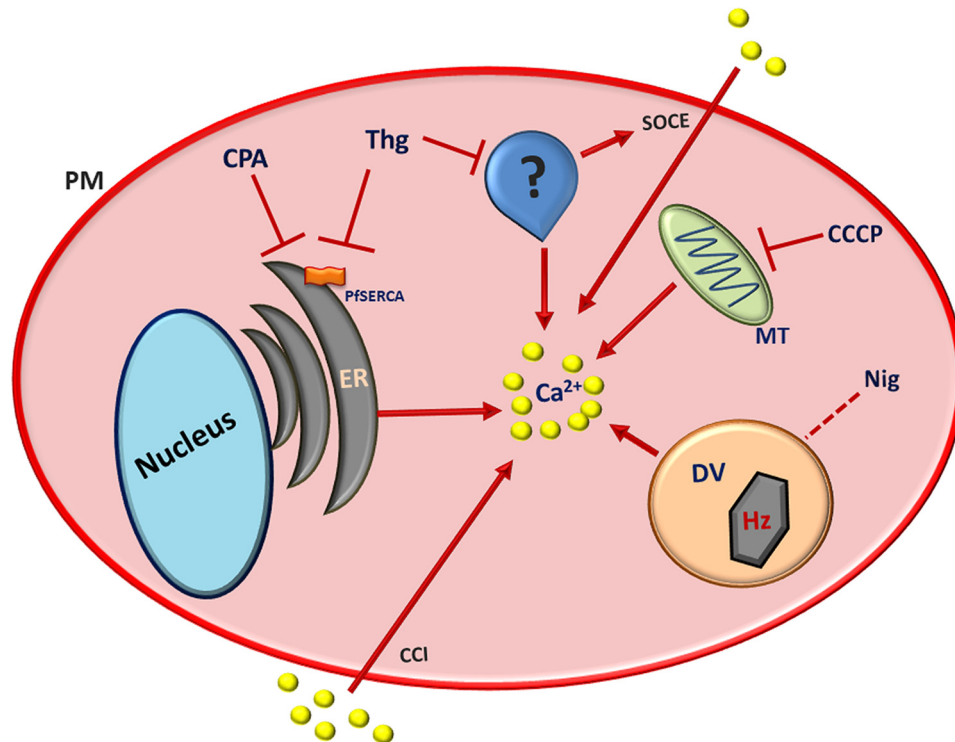
Figure 8. Proposed model for Thg action within *P. falciparum*. CPA and Thg are both able to release Ca^{2+} from the ER by inhibiting the *P. falciparum* SERCA (PfATP6). The presence of a Thg-Ca^{2+} response, even after emptying the ER with CPA, suggests that: (i) the two drugs target two intracellular Ca^{2+} pools, one sensitive to both SERCA inhibitors and one sensitive only to Thg; and (ii) alternatively the same Ca^{2+} pool could express two SERCA isoforms, one sensitive to both drugs and one sensitive only to Thg. If the latter is the case, the additional compartment was shown not to be the parasite mitochondrion or acidic pool. This additional compartment is crucial for SOCE in *P. falciparum*, because only Thg was able to activate Ca^{2+} influx into the parasite cytosol. *PM*, parasite plasma membrane; *MT*, mitochondrion; *DV*, digestive vacuole; *CCI*, constitutive Ca^{2+} influx; *Hz*, Hemozoin.

experiments to resolve the [Ca^{2+}]$_c$ increases with CPA and the Ca^{2+} ionophore A23187 (29). It is likely that this approach would miss the delayed asynchronous [Ca^{2+}]$_c$ oscillations observed with Thg in our imaging experiments. The slow action of Thg in imaging experiments presumably reflects the diffusion into the imaging chamber, the low solubility, and the need to accumulate relatively high concentrations of the drug within the parasite. The response to Thg in our cuvette system with rapid stirring is much faster.

The relatively low affinity for Thg-induced Ca^{2+} release raises the question of whether it acts on the same Ca^{2+} pump as CPA in *P. falciparum*. To address this question we carried out a series of experiments in which CPA and Thg were added sequentially, in both cell population cuvette experiments and single-cell imaging. These studies showed that pretreatment with Thg eliminated the response to subsequent CPA addition, whereas Thg was still able to cause a [Ca^{2+}]$_c$ increase after the Ca^{2+} response to a prior CPA addition was complete. In both cases there was no washout of the first drug prior to adding the second drug. Thus, it appears that Thg can release the same Ca^{2+} pool that is released by CPA. However, there is a second target for Thg, with a residual pool of Ca^{2+} still available for release after treatment with CPA. These data suggest two possibilities (Fig. 8): (i) the two drugs target two intracellular Ca^{2+} pools, one sensitive to both SERCA inhibitors and one only available for mobilization by Thg; and (ii) alternatively, the same Ca^{2+} pool could express two Ca^{2+} pumps, one sensitive to both drugs and one only affected by Thg. The latter case

would envision a store that requires the activity of both pumps to be fully loaded with Ca^{2+}, such that inhibition of only one leads to partial emptying, whereas inhibition of both pumps is required for complete Ca^{2+} release. In addition to PfATP6, a P-type ATPase gene, PfATP4, has been described in *P. falciparum* that has characteristics similar to those of eukaryotic P-type ATPases, in particular with conserved amino acids sequences involved in Ca^{2+} binding (43) and has also been reported to have Ca^{2+}-ATPase activity that is insensitive to low concentrations of Thg (44). However, PfATP4 is known to function as a plasma membrane sodium extrusion pump and has not been shown to transport Ca^{2+} (45, 46). Thus, it seems most likely that there is another, as-yet-unidentified target of Thg (47–50).

The fact that Thg causes Ca^{2+} oscillations, whereas CPA does not, points to a two-pool model for the action of Thg, rather than two Ca^{2+} pumps in the same ER store. For example, Thg might elicit Ca^{2+}-induced Ca^{2+} release from a pool that accumulates Ca^{2+} independent of SERCA activity. In the context of the possibility that Thg could act on a second Ca^{2+} store, distinct from the ER, we investigated the acidic compartment and the mitochondrion. The primary acidic Ca^{2+} compartment in *P. falciparum* is the digestive vacuole (23, 24), which appears to accumulate a relatively large load of Ca^{2+} in the isolated parasite preparation. We investigated the role of the acidic compartments in the actions of Thg and CPA using low levels of Nig. These experiments were carried out in the absence of extracellular Ca^{2+} to avoid any contribution from plasma membrane Ca^{2+} influx. Neither Thg nor CPA reduced the

amplitude of the Ca^{2+}-release response to Nig, even when measured with the low-affinity chemical indicator dye Fura-FF. Thus, these agents do not appear to deplete Ca^{2+} from the digestive vacuole, although we cannot rule out an effect of Thg on a minor acidic compartment that might be masked by the large Ca^{2+} release from the digestive vacuole.

We also examined a potential role of the mitochondrion using the uncoupler CCCP to collapse the mitochondrial membrane potential. In the presence of oligomycin to prevent reversal of the mitochondrial ATP synthase, CCCP did not cause any increase in $[Ca^{2+}]_c$ that would reflect Ca^{2+} loading of the *Plasmodium* mitochondrion in the intact parasite. Moreover, pretreatment with CCCP did not affect the ability of CPA or Thg to elicit Ca^{2+} responses. Thus, the mitochondrion does not represent an additional Ca^{2+} store sensitive to Thg.

We have previously shown that Thg activates a form of SOCE in *P. falciparum* and that this can be blocked by 2-aminoethyl diphenylborinate and its analogs (11). Significantly, this SOCE pathway is not activated by melatonin (11), which we have shown to elevate $[Ca^{2+}]_c$ by mobilizing an IP$_3$-linked Ca^{2+} pool in *Plasmodium* spp., believed to be the ER (4, 5). Therefore, in the present study we examined the $[Ca^{2+}]_c$ response to the SERCA inhibitors in the presence and absence of extracellular Ca^{2+}. Whereas the $[Ca^{2+}]_c$ increase elicited by CPA was always transient, Thg presented a distinct pattern of response in the two conditions, being sustained when extracellular Ca^{2+} was present and transient in the absence of Ca^{2+}. Moreover, only Thg increased the rate of Ca^{2+} entry when extracellular Ca^{2+} was added back after the depletion of intracellular stores. By contrast, CPA pretreatment had no effect on the rate of Ca^{2+} entry. It might be argued that CPA has a secondary effect to inhibit the SOCE. However, this does not appear to be the case, because Thg was able to activate SOCE whether it was added before or after CPA. The finding that Thg but not CPA can activate SOCE in *P. falciparum* is not necessarily incompatible with a one-pool model (Fig. 8), because it could be that complete emptying of the stores is required to activate SOCE (*i.e.* both the CPA/Thg-sensitive SERCA and the additional Thg-sensitive Ca^{2+} pump must be inhibited to reach a sufficiently low ER Ca^{2+} load). Nevertheless, the preponderance of the evidence seems most consistent with a two-pool model, in which CPA and Thg inhibit SERCA in a Ca^{2+}-containing ER compartment, and there is an additional Ca^{2+}-containing intracellular compartment that is specifically mobilized by Thg. This would best explain the different patterns of $[Ca^{2+}]_c$ response observed with Thg and CPA and the observation that only Thg can activate the SOCE-like Ca^{2+} influx in *P. falciparum*.

The intraerythrocytic trophozoite phase malaria parasite is sequestered within the parasitophorous vacuole inside the RBC, and this might be expected to preclude significant SOCE because RBC cytosolic Ca^{2+} is maintained in the nanomolar range. However, the parasitophorous vacuole is formed by invagination of the red cell plasma membrane, and we have previously shown that Ca^{2+} within the vacuole is at least 2 orders of magnitude higher than in the parasite or RBC cytosol (35). This elevated Ca^{2+} level could be maintained by a parasitophorous duct connecting the vacuole to the extraerythrocytic me-

dium (51) or through Ca^{2+} transport into the vacuole by plasma membrane-derived RBC Ca^{2+} pumps. Thus, SOCE at the trophozoite stage can play a physiological role and may be required to maintain Ca^{2+} signaling and parasite maturation during this phase of the life cycle (11, 35). It is also possible that the *P. falciparum* SOCE participates in Ca^{2+} signaling during egress of the mature parasite as the RBC membranes break down and during the invasion of new RBCs by the extracellular merozoites. In mammalian cells SOCE is mediated by STIM and Orai proteins, which have no homologs in the *P. falciparum* genome. Thus, in *Plasmodium*, the SOCE-like process most likely occurs through molecular mechanisms different from those described in mammals or through functional analogs of STIM and Orai that are molecularly distinct.

Experimental procedures

P. falciparum: culture, synchronization, and isolation of parasites

P. falciparum was maintained in continuous culture as previously described (52). A novel, transgenic strain of *P. falciparum* (derived from 3D7) expressing the genetically encoded Ca^{2+} indicator GCaMP3 (PfGCaMP3) was used for all of the experiments in this paper. This clone was developed by Borges-Pereira *et al.* (32). Briefly, GCaMP3 (a gift from Loren Looger (34); Addgene plasmid no. 22692) was cloned and inserted into the *P. falciparum* expression vector pDC and then transfected into trophozoite phase parasites via electroporation. Episomal vector expression is maintained by the continuous presence of the selection agent (WR99210; 5 nM). The parasites were grown in plastic cell culture flasks (175 cm²) with RPMI 1640 medium (GibcoBRL) supplemented with 0.5% AlbuMAX I (Gibco) and 5 nM of WR99210 with 5% hematocrit in a 90% N$_2$; 5% O$_2$; 5% CO$_2$ atmosphere at 37 °C. The parasites were synchronized ~12–18 h prior to isolation via sorbitol treatment (53) to yield a homogenous population of trophozoite stage parasites, as verified by Giemsa-stained thin blood smears. Synchronized cells were pelleted, resuspended into PBS. Free parasites were isolated from the RBCs by saponin treatment (0.01%), which eliminates the RBC plasma membrane and parasitophorous vacuole, without disrupting the integrity of the parasite plasma membrane (54). The trophozoite stage parasites were collected by centrifugation at 2,000 rpm and washed twice into a MOPS-based buffer (116 mM NaCl, 5.4 mM KCl, 0.8 mM MgSO$_4$, 2 mM CaCl$_2$, 5.5 mM D-glucose, 50 mM MOPS, pH 7.2) or HEPES-based imaging buffer (25 mM HEPES, 121 mM NaCl, 5 mM NaHCO$_3$, 4.7 mM KCl, 1.2 mM KH$_2$PO$_4$, 1.2 mM MgSO$_4$, 2 mM CaCl$_2$, 10 mM glucose, 0.25% BSA, pH 7.4).

Spectrofluorometric determinations

Isolated parasites at the trophozoite stage were used to perform experiments either in the presence or absence of extracellular Ca^{2+} (no CaCl$_2$ added plus addition of 100 μM EGTA). Cytosolic Ca^{2+} dynamics after addition of the compounds were monitored using a Shimadzu spectrofluorometer (RF5301PC, Japan) with parasites (10^7 cells ml^{-1}) in a 1-ml stirred cuvette. Excitation of GCaMP3 fluorescence was performed at 488 nm, and emission was measured at 530 nm. All assays were

performed at 37 °C, in triplicate, with at least three independent experiments.

The Ca^{2+} dose response of isolated parasites to CPA was also measured in a FlexStation 3 plate spectrofluorometer (Molecular Devices). For this, 96-well plates (black with a clear, flat bottom) were treated overnight with 50 μg of poly-L-lysine. Isolated PfGCaMP3 parasites at trophozoite stage were added to each plate well (10^7/well in 200 μl total volume) and incubated for ∼30 min, allowing parasite adhesion to the plate bottom. After this, the medium was replaced to remove the parasites that did not adhere. Cytosolic Ca^{2+} dynamics after addition of CPA was monitored in the 96-well plate spectrofluorometer using the multichannel fluidic addition capabilities. GCaMP3 was excited at 488 nm, and emission was measured at 530 nm.

Fluorescence imaging

Isolated parasites were plated onto borosilicate glass coverslips coated with Cell-Tak via the adsorption method according to the manufacturer's instructions (Sigma) and allowed to settle for 30 min at 37 °C to enable cell adherence. Once plated, the coverslips were washed twice and mounted in a 37 °C temperature-controlled cell chamber with 3 ml of imaging buffer on the stage of a wide-field epifluorescence inverted microscope (Nikon Eclipse TE300). Imaging was performed using a heated 40× oil immersion objective and an EM-CCD camera (Hamamatsu Photonix ImageEM); GCaMP3 images (excitation, 488 nm; emission, 510 nm; long band pass filter) were acquired at 1 Hz using the data acquisition software NIS Elements (Nikon).

Ca²⁺ influx measurements

Immediately prior to imaging, the parasites were switched into a modified imaging buffer without Ca^{2+} supplemented with 100 μM EGTA. The cells were then treated with either CPA (10 μM, Cayman Chem Co.), Thg (5 μM, Cayman Chem Co.), or vehicle control (DMSO) for 10 min prior to Ca^{2+} add-back.

Mitochondrial membrane potential

TMRE was used to determine the concentration of the mitochondrial uncoupler carbonyl cyanide 3-chlorophenylhydrazone (CCCP) required to cause complete dissipation of the mitochondrial membrane potential. Images of TMRE fluorescence were obtained using 543-nm excitation and 580-nm emission and were acquired at 1 Hz. The isolated parasites were loaded with TMRE (5 nM, Sigma) for 13 min, followed by treatment with CCCP (2.5 μM, Sigma) and oligomycin (2.5 μg·ml^{-1}, Sigma).

Analysis

Imaging data were acquired and processed using NIS Elements (Nikon) software and analyzed using a custom in-house program built in MATLAB. The data were normalized to the maximum ionomycin Ca^{2+} response (F/F_{Iono}). Statistical analysis was performed in GraphPad Prism, including one-way ANOVA testing with Bonferroni's multiple comparison test.

Data availability

All data are contained within the article and the accompanying supporting information.

Conflict of interest—The authors declare that they have no conflicts of interest with the contents of this article.

Abbreviations—The abbreviations used are: CCCP, carbonyl cyanide 3-chlorophenylhydrazone; CPA, cyclopiazonic acid; GECI genetically encoded calcium indicator; IP₃, inositol 1,4,5-trisphosphate; ER, endoplasmic reticulum; SR, sarcoplasmic reticulum; SERCA, sarcoplasmic/endoplasmic reticulum Ca^{2+}-ATPase; SOCE, store-operated calcium entry; TMRE, tetramethylrhodamine ethyl ester; Thg, thapsigargin; Nig, nigericin; RBC, red blood cell; ANOVA, analysis of variance.

References

1. WHO/UNICEF (2016) WHO/UNICEF report: malaria MDG target achieved amid sharp drop in cases and mortality, but 3 billion people remain at risk. *Neurosciences (Riyadh)* **21,** 87–88 Medline
2. Berridge, M. J., Lipp, P., and Bootman, M. D. (2000) The versatility and universality of calcium signalling. *Nat. Rev. Mol. Cell. Biol.* **1,** 11–21 CrossRef Medline
3. Budu, A., and Garcia, C. R. (2012) Generation of second messengers in *Plasmodium. Microbes Infect.* **14,** 787–795 CrossRef Medline
4. Hotta, C. T., Gazarini, M. L., Beraldo, F. H., Varotti, F. P., Lopes, C., Markus, R. P., Pozzan, T., and Garcia, C. R. (2000) Calcium-dependent modulation by melatonin of the circadian rhythm in malarial parasites. *Nat. Cell Biol.* **2,** 466–468 CrossRef Medline
5. Alves, E., Bartlett, P. J., Garcia, C. R., and Thomas, A. P. (2011) Melatonin and IP₃-induced Ca^{2+} release from intracellular stores in the malaria parasite *Plasmodium falciparum* within infected red blood cells. *J. Biol. Chem.* **286,** 5905–5912 CrossRef Medline
6. Enomoto, M., Kawazu, S., Kawai, S., Furuyama, W., Ikegami, T., Watanabe, J., and Mikoshiba, K. (2012) Blockage of spontaneous Ca^{2+}

oscillation causes cell death in intraerythrocitic *Plasmodium falciparum.* *PLoS One* **7,** e39499 CrossRef Medline

7. Kumar, P., Tripathi, A., Ranjan, R., Halbert, J., Gilberger, T., Doerig, C., and Sharma, P. (2014) Regulation of *Plasmodium falciparum* development by calcium-dependent protein kinase 7 (PfCDPK7). *J. Biol. Chem.* **289,** 20386–20395 CrossRef Medline

8. Singh, S., Alam, M. M., Pal-Bhowmick, I., Brzostowski, J. A., and Chitnis, C. E. (2010) Distinct external signals trigger sequential release of apical organelles during erythrocyte invasion by malaria parasites. *PLoS Pathogens* **6,** e1000746 CrossRef Medline

9. Weiss, G. E., Gilson, P. R., Taechalertpaisarn, T., Tham, W.-H., de Jong, N. W. M., Harvey, K. L., Fowkes, F. J. I., Barlow, P. N., Rayner, J. C., Wright, G. J., Cowman, A. F., and Crabb, B. S. (2015) Revealing the sequence and resulting cellular morphology of receptor–ligand interactions during *Plasmodium falciparum* invasion of erythrocytes. *PLoS Pathogens* **11,** e1004670 CrossRef Medline

10. Levano-Garcia, J., Dluzewski, A. R., Markus, R. P., and Garcia, C. R. S. (2010) Purinergic signalling is involved in the malaria parasite *Plasmodium falciparum* invasion to red blood cells. *Purinergic Signal.* **6,** 365–372 CrossRef Medline

11. Pecenin, M. F., Borges-Pereira, L., Levano-Garcia, J., Budu, A., Alves, E., Mikoshiba, K., Thomas, A., and Garcia, C. R. S. (2018) Blocking IP$_3$ signal transduction pathways inhibits melatonin-induced Ca^{2+} signals and impairs *P. falciparum* development and proliferation in erythrocytes. *Cell Calcium* **72,** 81–90 CrossRef Medline

12. Cheemadan, S., Ramadoss, R., and Bozdech, Z. (2014) Role of calcium signaling in the transcriptional regulation of the apicoplast genome of *Plasmodium falciparum. Biomed Res. Int.* **2014,** 869401 CrossRef Medline

13. Lourido, S., and Moreno, S. N. (2015) The calcium signaling toolkit of the Apicomplexan parasites *Toxoplasma gondii* and *Plasmodium* spp. *Cell Calcium* **57,** 186–193 CrossRef Medline

14. Pizzo, P., Lissandron, V., Capitanio, P., and Pozzan, T. (2011) Ca^{2+} signalling in the Golgi apparatus. *Cell Calcium* **50,** 184–192 CrossRef Medline

15. Michelangeli, F., and East, J. M. (2011) A diversity of SERCA Ca^{2+} pump inhibitors. *Biochem. Soc. Trans.* **39,** 789–797 CrossRef Medline

16. Lai, P., and Michelangeli, F. (2012) Bis(2-hydroxy-3-*tert*-butyl-5-methyl-phenyl)-methane (bis-phenol) is a potent and selective inhibitor of the secretory pathway Ca^{2+} ATPase (SPCA1.). *Biochem. Biophys. Res. Commun.* **424,** 616–619 CrossRef Medline

17. Wong, A. K., Capitanio, P., Lissandron, V., Bortolozzi, M., Pozzan, T., and Pizzo, P. (2013) Heterogeneity of Ca^{2+} handling among and within Golgi compartments. *J Mol. Cell Biol.* **5,** 266–276 CrossRef Medline

18. Melchionda, M., Pittman, J. K., Mayor, R., and Patel, S. (2016) Ca^{2+}/H$^+$ exchange by acidic organelles regulates cell migration *in vivo. J. Cell Biol.* **212,** 803–813 CrossRef Medline

19. Patel, S., and Docampo, R. (2010) Acidic calcium stores open for business: expanding the potential for intracellular Ca^{2+} signaling. *Trends Cell Biol.* **20,** 277–286 CrossRef Medline

20. Docampo, R., de Souza, W., Miranda, K., Rohloff, P., and Moreno, S. N. (2005) Acidocalcisomes: conserved from bacteria to man. *Nat. Rev. Microbiol.* **3,** 251–261 CrossRef Medline

21. Vercesi, A. E., Moreno, S. N., and Docampo, R. (1994) Ca^{2+}/H$^+$ exchange in acidic vacuoles of *Trypanosoma brucei. Biochem. J.* **304,** 227–233 CrossRef Medline

22. Brochet, M., and Billker, O. (2016) Calcium signalling in malaria parasites. *Mol. Microbiol.* **100,** 397–408 CrossRef Medline

23. Biagini, G. A., Bray, P. G., Spiller, D. G., White, M. R., and Ward, S. A. (2003) The digestive food vacuole of the malaria parasite is a dynamic intracellular Ca^{2+} store. *J. Biol. Chem.* **278,** 27910–27915 CrossRef Medline

24. Rohrbach, P., Friedrich, O., Hentschel, J., Plattner, H., Fink, R. H., and Lanzer, M. (2005) Quantitative calcium measurements in subcellular compartments of *Plasmodium falciparum*–infected erythrocytes. *J. Biol. Chem.* **280,** 27960–27969 CrossRef Medline

25. Varotti, F. P., Beraldo, F. H., Gazarini, M. L., and Garcia, C. R. (2003) *Plasmodium falciparum* malaria parasites display a THG-sensitive Ca^{2+} pool. *Cell Calcium* **33,** 137–144 CrossRef Medline

26. Eckstein-Ludwig, U., Webb, R. J., Van Goethem, I. D., East, J. M., Lee, A. G., Kimura, M., O'Neill, P. M., Bray, P. G., Ward, S. A., and Krishna, S. (2003) Artemisinins target the SERCA of *Plasmodium falciparum. Nature* **424,** 957–961 CrossRef Medline

27. Gomes, M. M., Budu, A., Ventura, P. D., Bagnaresi, P., Cotrin, S. S., Cunha, R. L., Carmona, A. K., Juliano, L., and Gazarini, M. L. (2015) Specific calpain activity evaluation in *Plasmodium* parasites. *Anal. Biochem.* **468,** 22–27 CrossRef Medline

28. Alleva, L. M., and Kirk, K. (2001) Calcium regulation in the intraerythrocytic malaria parasite *Plasmodium falciparum. Mol. Biochem. Parasitol.* **117,** 121–128 CrossRef Medline

29. Pandey, K., Ferreira, P. E., Ishikawa, T., Nagai, T., Kaneko, O., and Yahata, K. (2016) Ca^{2+} monitoring in *Plasmodium falciparum* using the yellow cameleon–Nano biosensor. *Sci. Rep.* **6,** 23454 CrossRef Medline

30. Arnou, B., Montigny, C., Morth, J. P., Nissen, P., Jaxel, C., Møller, J. V., and Maire, M. (2011) The *Plasmodium falciparum* Ca^{2+}-ATPase PfATP6: insensitive to artemisinin, but a potential drug target. *Biochem. Soc. Trans.* **39,** 823–831 CrossRef Medline

31. Borges-Pereira, L., Budu, A., McKnight, C. A., Moore, C. A., Vella, S. A., Hortua Triana, M. A., Liu, J., Garcia, C. R., Pace, D. A., and Moreno, S. N. (2015) Calcium signaling throughout the *Toxoplasma gondii* lytic cycle: a study using genetically encoded calcium indicators. *J. Biol. Chem.* **290,** 26914–26926 CrossRef Medline

32. Borges-Pereira, L., Campos, B. R., and Garcia, C. R. (2014) The GCaMP3: a GFP-based calcium sensor for imaging calcium dynamics in the human malaria parasite *Plasmodium falciparum. MethodsX* **1,** 151–154 CrossRef Medline

33. Tian, L., Hires, S. A., and Looger, L. L. (2012) Imaging neuronal activity with genetically encoded calcium indicators. *Cold Spring Harb. Protoc.* **2012,** 647–656 Medline CrossRef Medline

34. Tian, L., Hires, S. A., Mao, T., Huber, D., Chiappe, M. E., Chalasani, S. H., Petreanu, L., Akerboom, J., McKinney, S. A., Schreiter, E. R., Bargmann, C. I., Jayaraman, V., Svoboda, K., and Looger, L. L. (2009) Imaging neural activity in worms, flies and mice with improved GCaMP calcium indicators. *Nat. Methods* **6,** 875–881 CrossRef Medline

35. Gazarini, M. L., Thomas, A. P., Pozzan, T., and Garcia, C. R. (2003) Calcium signaling in a low calcium environment: how the intracellular malaria parasite solves the problem. *J. Cell Biol.* **161,** 103–110 CrossRef Medline

36. Furuyama, W., Enomoto, M., Mossaad, E., Kawai, S., Mikoshiba, K., and Kawazu, S. (2014) An interplay between 2 signaling pathways: melatonin–cAMP and IP3–Ca^{2+} signaling pathways control intraerythrocytic development of the malaria parasite *Plasmodium falciparum. Biochem. Biophys. Res. Commun.* **446,** 125–131 CrossRef Medline

37. Borges-Pereira, L., and Garcia, C. R. S. (2019) Employing transgenic parasite strains to study the Ca^{2+} dynamics in the human malaria parasite *Plasmodium falciparum. Methods Mol. Biol.* **1925,** 157–162 CrossRef Medline

38. Garcia, C. R. S., Alves, E., Pereira, P. H. S., Bartlett, P. J., Thomas, A. P., Mikoshiba, K., Plattner, H., and Sibley, L. D. (2017) InsP3 signaling in apicomplexan parasites. *Curr. Top. Med. Chem.* **17,** 2158–2165 CrossRef Medline

39. Yayon, A., Cabantchik, Z. I., and Ginsburg, H. (1984) Identification of the acidic compartment of *Plasmodium falciparum*–infected human erythrocytes as the target of the antimalarial drug chloroquine. *EMBO J.* **3,** 2695–2700 CrossRef Medline

40. Gazarini, M. L., and Garcia, C. R. (2004) The malaria parasite mitochondrion senses cytosolic Ca^{2+} fluctuations. *Biochem. Biophys. Res. Commun.* **321,** 138–144 CrossRef Medline

41. Passos, A. P., and Garcia, C. R. (1998) Inositol 1,4,5-trisphosphate induced Ca^{2+} release from chloroquine-sensitive and -insensitive intracellular stores in the intraerythrocytic stage of the malaria parasite *P. chabaudi. Biochem. Biophys. Res. Commun.* **245,** 155–160 CrossRef Medline

42. Kawamoto, F., Fujioka, H., Murakami, R. I., Syafruddin, Hagiwara, M., Ishikawa, T., and Hidaka, H. (1993) The roles of Ca^{2+} calmodulin–dependent and cGMP-dependent pathways in gametogenesis of a rodent

malaria parasite, *Plasmodium berghei. Eur. J. Cell Biol*. **60,** 101–107 Medline

43. Trottein, F., Thompson, J., and Cowman, A. F. (1995) Cloning of a new cation ATPase from *Plasmodium falciparum*: conservation of critical amino acids involved in calcium binding in mammalian organellar Ca^{2+}-ATPases. *Gene* **158,** 133–137 CrossRef Medline

44. Krishna, S., Woodrow, C., Webb, R., Penny, J., Takeyasu, K., Kimura, M., and East, J. M. (2001) Expression and functional characterization of a *Plasmodium falciparum* Ca^{2+}-ATPase (PfATP4) belonging to a subclass unique to apicomplexan organisms. *J. Biol. Chem*. **276,** 10782–10787 CrossRef Medline

45. Spillman, N. J., Allen, R. J., McNamara, C. W., Yeung, B. K., Winzeler, E. A., Diagana, T. T., and Kirk, K. (2013) Na$^+$ regulation in the malaria parasite *Plasmodium falciparum* involves the cation ATPase PfATP4 and is a target of the spiroindolone antimalarials. *Cell Host Microbe* **13,** 227–237 CrossRef Medline

46. Rosling, J. E. O., Ridgway, M. C., Summers, R. L., Kirk, K., and Lehane, A. M. (2018) Biochemical characterization and chemical inhibition of PfATP4-associated Na$^+$-ATPase activity in *Plasmodium falciparum* membranes. *J. Biol. Chem*. **293,** 13327–13337 CrossRef Medline

47. Kenthirapalan, S., Waters, A. P., Matuschewski, K., and Kooij, T. W. (2016) Functional profiles of orphan membrane transporters in the life cycle of the malaria parasite. *Nat. Commun.* **7,** 10519 CrossRef Medline

48. Krishna, S., Cowan, G., Meade, J. C., Wells, R. A., Stringer, J. R., and Robson, K. J. (1993) A family of cation ATPase-like molecules from *Plasmodium falciparum. J. Cell Biol*. **120,** 385–398 CrossRef Medline

49. Martin, R. E., Henry, R. I., Abbey, J. L., Clements, J. D., and Kirk, K. (2005) The "permeome" of the malaria parasite: an overview of the membrane transport proteins of *Plasmodium falciparum. Genome Biol*. **6,** R26 CrossRef Medline

50. Rozmajzl, P. J., Kimura, M., Woodrow, C. J., Krishna, S., and Meade, J. C. (2001) Characterization of P-type ATPase 3 in *Plasmodium falciparum. Mol. Biochem. Parasitol*. **116,** 117–126 CrossRef Medline

51. Pouvelle, B., Spiegel, R., Hsiao, L., Howard, R. J., Morris, R. L., Thomas, A. P., and Taraschi, T. F. (1991) Direct access to serum macromolecules by intraerythrocytic malaria parasites. *Nature* **353,** 73–75 CrossRef Medline

52. Trager, W., and Jensen, J. B. (1976) Human malaria parasites in continuous culture. *Science* **193,** 673–675 CrossRef Medline

53. Lambros, C., and Vanderberg, J. P. (1979) Synchronization of *Plasmodium falciparum* erythrocytic stages in culture. *J. Parasitol*. **65,** 418–420 CrossRef Medline

54. Ansorge, I., Benting, J., Bhakdi, S., and Lingelbach, K. (1996) Protein sorting in *Plasmodium falciparum*–infected red blood cells permeabilized with the pore-forming protein streptolysin O. *Biochem. J*. **315,** 307–314 CrossRef Medline